Innovative Food Science and Emerging Technologies 82 (2022) 103181

Contents lists available at ScienceDirect

Innovative Food Science and Emerging Technologies

journal homepage: www.elsevier.com/locate/ifset

Preparation of nano/microcapsules of ozonated olive oil in chitosan matrix and analysis of physicochemical and microbiological properties of the obtained films

Nikola Nowak [a], Wiktoria Grzebieniarz [a], Gohar Khachatryan [a], Anna Konieczna-Molenda [a], Marcel Krzan [b], Karen Khachatryan [a,*]

[a] Faculty of Food Technology, University of Agriculture in Krakow, Balicka Str. 122, 30-149 Krakow, Poland
[b] Jerzy Haber Institute of Catalysis and Surface Chemistry, Polish Academy of Sciences, Niezapominajek Str. 8, 30-239 Krakow, Poland

ARTICLE INFO

Keywords:
Nanocapsules
Ozonated olive oil
Chitosan
Active packaging
Biopolymer films
Enzymatic hydrolysis

ABSTRACT

In order to meet one of the greatest problems of food technology, i.e. unwanted food spoilage caused by the action of microorganisms, active or intelligent packaging is being created and used with increasing frequency. At the same time, substitutes for plastics are being sought in order to protect the environment. Biodegradable polymer composites seem to be an extremely promising material that could replace synthetic materials in the future. By encapsulating biologically active substances in a polymer matrix, directional action and controlled release of the substance are possible. The use of ozone, which has become more and more popular especially recently, allows to limit the growth of microorganisms, and the production of ozone derivatives of unsaturated fats allows to reduce the short time of its decomposition.

The aim of this study was to analyse the physicochemical and bacteriostatic properties of innovative chitosan-based films containing encapsulated nanocapsules of ozonated olive oil in two concentrations. The morphology and size of the obtained nanocapsules were determined using Scanning Electron Microscopy and DLS. The largest particle size was observed for the film containing the lower ozone concentration – up to 4900 nm, in the control film 3500 nm, for the film with the highest ozone concentration, the particle size was the smallest, with the majority in the range of 100–1000 nm. Ozone content was determined by peroxidation number. The properties of the composites were characterised by infrared (IR) which proved that chitosan is a good matrix for the formation of capsules and ultraviolet (UV) which showed that the obtained composite absorbs light in the range of blue and near ultraviolet light, and the addition of nanocapsules of ozonated olive oil increased the degree of absorption and decreased the transparency. We also performed photoluminescence spectroscopy before and after storage of pork meat proving that films are sensitive to the physico-chemical and biochemical transformation products formed as a result of meat spoilage. The study of the microbiological properties included the analysis of the microbiological quality of pork meat stored under the obtained films as a function of time. The films have a bactericidal and bacteriostatic effect and the addition of ozonated olive oil capsules increases the bactericidal effect against Gram-negative bacteria. Contact angles, Water Vapour Transmission Rate and transparency were also determined and they were subjected to enzymatic hydrolysis. Water absorption, solubility and liquid absorption capacity were determined. All tested samples show high hydrophobicity and low solubility, and the ozone content directly influences these parameters.

1. Introduction

Apart from global warming, one of the most serious challenges facing the world today is the logarithmically growing population. This poses not only economic and environmental challenges, but also social, medical and in terms of food. Food problems can be solved in two ways. One way is to produce as much food as possible in an optimised way, while the other focusses on the long-term effects by optimising

* Corresponding author.
E-mail addresses: nikola.nowak@urk.edu.pl (N. Nowak), wiktoria.grzebieniarz@urk.edu.pl (W. Grzebieniarz), gohar.khachatryan@urk.edu.pl (G. Khachatryan), anna.konieczna-molenda@urk.edu.pl (A. Konieczna-Molenda), marcel.krzan@ikifp.edu.pl (M. Krzan), karen.khachatryan@urk.edu.pl (K. Khachatryan).

https://doi.org/10.1016/j.ifset.2022.103181
Received 21 February 2022; Received in revised form 11 July 2022; Accepted 7 October 2022
Available online 13 October 2022

packaging and food safety, and biodegradable films belong to this trend. Biodegradable films are not only a solution for the ecological problem of the use of synthetic materials, but also to the challenges posed to food technology and medicine. Biodegradable composites are also used as carriers of biologically active substances or substances with antimicrobial properties (Bilal & Iqbal, 2019; Rozilah, Aiza Jaafar, Sapuan, Zainol, & Ilyas, 2020; Udayakumar et al., 2021; Yahya et al., 2020). Recent events related to the Sars CoV-2 coronavirus pandemic have made us aware of the importance of food safety. The encapsulation of biologically active substances in a polymer matrix extends the shelf life of a product through antimicrobial activity or protection against harmful UV radiation, but could also potentially ensure consumer safety by preventing survival or growth of pathogens on its surface (Adeyeye et al., 2019; Gabor & Tita, 2012; Garavand, Rouhi, Razavi, Cacciotti, & Mohammadi, 2017; Grujić et al., 2017).

Due to its properties, chitosan is a popular polymer used to produce biodegradable packaging. After starch and cellulose, chitosan is the second most common polymer found in nature, with antibacterial properties and the ability to form membranes. It is used in many fields such as medicine, tissue engineering, biomaterials and biosensors (B. Li et al., 2015; Wang et al., 2017; Yu, Li, Chu, & Zhang, 2018). Using chitosan as a matrix for encapsulating biologically active substances improves its natural properties while maintaining environmental neutrality of the composite components. Nanoencapsulation is a method of trapping a substance in a polymer, which uses the most important and greatest principle of nanotechnology, i.e. obtaining the same or often better properties of a substance with the use of extremely small quantities of substances (Arora & Padua, 2010; Gabor & Tita, 2012; Grujić et al., 2017; Sarkar et al., 2022).

Many descriptions of the addition of active natural ingredients or nanoparticles such as metal nanoparticles (Amjadi et al., 2019) to improve the functional properties of biopolymer films are available in the literature (Bahrami, Delshadi, Assadpour, Jafari, & Williams, 2020). The functional properties of the film are, among others, influenced by its mechanical strength, ability to inhibit microbial growth or water vapour permeability-. Many attempts to add essential oils as natural hydrophobic components have been described, which positively influence the above-mentioned properties (Amjadi, Almasi, Ghorbani, & Ramazani, 2020; Atarés & Chiralt, 2016; Varghese, Siengchin, & Parameswaranpillai, 2020), but do not show strong bactericidal activity, or only selective (Almasi, Radi, Amiri, & McClements, 2021; Khah, Ghanbarzadeh, Roufegarinejad Nezhad, & Ostadrahimi, 2021). A further enlightenment of the use of essential oils as packaging additives is their effect on the taste and smell of food (Marangoni Júnior, Vieira, Jamróz, & Anjos, 2021; Yong & Liu, 2021). The use of nanometals, although in trace amounts, also has its opponents - due to uncertainty about the accumulation of metals in the body or the eventual use of environmentally harmful compounds such as cadmium (Elsamadony et al., 2021; Ganguly, Breen, & Pillai, 2018; Zhu et al., 2019). These limitations are one of the many reasons for the further search for biopolymer films and active ingredients additives, which in the future could successfully replace the use of plastics in packaging.

In the present study, the polymer used to obtain the composite is chitosan and the nanoencapsulated substance is ozonated olive oil. In recent months, ozone has gained particular popularity due to its strong oxidising properties but also its strong inactivating effect against viruses. It is commonly used as an effective method for disinfection of surfaces, water and air in potentially contaminated rooms (Bayarri, Cruz-Alcalde, López-Vinent, Micó, & Sans, 2021; Habibi Najafi & Haddad Khodaparast, 2009; Hudson, Sharma, & Vimalanathan, 2009; C. S. Li & Wang, 2010). An analysis of literature data on the antiviral efficacy of ozone has shown that when used in low concentrations it is 99% effective (bacteriophage Φ6, bacteriophage Φ X174, bacteriophage MS2 and bacteriophage T7 required ozone of 1.43 ppm, 1.90 ppm, 2.90 ppm, and 5.12 ppm, respectively at the time 18.4 s) (Tseng & Li, 2006). The only limitation in its use seems to be its potential negative health effects on humans, as it can cause inflammation and deterioration of lung function, but also the fact that ozone is an unstable gas. In order to prolong the relatively short decomposition time of ozone, ozonated derivatives of unsaturated fats (vegetable oils) have been produced using its ability to bond with the double bonds of unsaturated fatty acids. The olive oil used in this study consists of 90% oleic acid and therefore has a high degree of unsaturation, which makes it perfect for ozone bonding, ensuring a longer gas shelf life (Pastor, Sánchez-González, Chiralt, Cháfer, & González-Martínez, 2013; Sadowska et al., 2008; Ugazio, Tullio, Binello, Tagliapietra, & Dosio, 2020).

The aim of this study was to develop and analyse a chitosan-based composite containing nanocapsules of ozonated olive oil at two concentrations. Scanning Electron Microscopy and Dynamic Light Scattering (DLS) were performed to characterise the obtained nanocapsules. Physicochemical analysis of the composites included UV–Vis spectrophotometry, and FTIR – ATR and photoluminescence spectroscopy. Contact angles were determined and the films were subjected to enzymatic and acid hydrolysis. The water content, solubility liquid absorption capacity and water vapour barrier properties of the composites studied were determined. The study of the microbiological properties included an analysis of the microbiological quality of pork stored for 4 days under the obtained films in refrigeration conditions. The pieces of meat were stored in sterile plastic containers and analysed for the samples (K, 03–0.5 and 03–1) and for the polyethylene stretch foil for food packaging (FS) by placing a piece of analysed, sterilised film in the cap.

2. Materials and methods

2.1. Materials

Chitosan from shrimp shells, high molecular weight: 310,000–375,000 Da, degree of deacetylation >75% (Sigma-Aldrich, St. Louis, MO, USA, CAS number 9012-76-4), acetic acid (99.5%, Sigma-Aldrich, St. Louis, MO, USA, CAS number 64–19-7), glycrol (99.5%, Sigma-Aldrich, St. Louis, MO, USA, CAS number 56–81-5) and ozonated olive oil (Scandia Cosmetics S.A., Niepołomice, Poland) with an ozone content of 1.11 ± 0.02 g in 100 g of oil were used to produce the nanocomposite.

2.2. Preparation of polymer matrix

750 g of 2% chitosan solution was prepared by dissolving 15 g of chitosan in 735 ml of 0.5% acetic acid solution. The solution was then placed in a magnetic stirrer (Heidolph RZR 2020) and stirred at 70 degrees Celsius until the chitosan was completely dissolved. During gelation, 7.5 g of glycerol was added as a plasticiser.

2.3. Determination of ozone content

The ozone content of the vegetable oils used and the products obtained was determined by the peroxidation number according to the procedure described in the European Pharmacopoeia (European Pharmacopoeia, *2019*).

2.4. Emulsification of ozonised olive oil

To obtain the nanoemulsion, a mixture of water and ozonated olive oil in a weight ratio of 1:1 was placed for 25 min in an ultrasonic bath (Polsonic, Sonic 10) at the temperature of 10 °C, power of sonification 2 × 400 W and frequency 40 kHz.

2.5. Preparation of the control sample (K)

From the prepared polymer matrix, 250 g was poured into a beaker, then 8 ml water was added and placed on a magnetic stirrer (Heidolph

RZR 2020). The mixture was left to stir vigorously for 15 min and then 100 g of gel was poured into sterile 12 cm diameter polypropylene pans. The film was allowed to dry at room temperature to form a film. After drying the films were stored in a tightly closed zipper bag at room temperature.

2.6. Sample preparation O_3_0.5

From the prepared polymer matrix, 250 g were poured into a beaker, then 4 ml water was added and placed on a magnetic stirrer (Heidolph RZR 2020). While stirring vigorously, 4 ml of the resulting emulsion was slowly added dropwise and left for 15 min on the stirrer. After stirring, 100 g of gel was poured into sterile polypropylene pans of 12 cm diameter. The film was allowed to dry at room temperature to form a film. After drying the films were stored in a tightly closed zipper bag at room temperature.

2.7. Sample preparation O_3_1.0

From the prepared polymer matrix, 250 g were poured into a beaker and placed on a magnetic stirrer (Heidolph RZR 2020). While stirring vigorously, 8 ml of the resulting emulsion was slowly added dropwise and left for 15 min on the stirrer. After stirring, 100 g of gel was poured into sterile polypropylene pans of 12 cm diameter. The film was allowed to dry at room temperature to form a film. After drying the films were stored in a tightly closed zipper bag at room temperature. The schematic diagram of preparation of nanocomposite films is shown in Fig. 1.

2.8. Scanning electron microscopy (SEM)

The size and morphology of the nanoparticles thus prepared were analysed using a JEOL 7550 (Akishima, Tokyo, Japan) scanning electron microscope. Before the measurement, the prepared sapmples were sprayed (K575X Turbo Sputter Coater) with 20 nm of chromium to increase a conductivity of the samples.

2.9. UV–Vis spectrophotometry

UV–Vis absorption spectra of the composites obtained were analysed in the range of 200–800 nm using a Shimadzu 2101 (Shimadzu, Kyoto, Japan) scanning spectrophotometer.

2.10. FTIR-ATR spectroscopy

FTIR-ATR spectra of the composites were recorded in the 4000–700 cm^{-1} range at 4 cm^{-1} resolution using a MATTSON 3000 FTIR spectrophotometer (Madison, Wisconsin, USA) equipped with a 30SPEC 30 Degree Reflectance adapter (MIRacle ATR, PIKE Technologies Inc., Madison, Wisconsin, USA).

2.11. Determination of water content, solubility and liquid absorption capacity

Water content, solubility and liquid absorption capacity were determined according to Pastor et al.(Pastor et al., 2013) and Peng and Li (Peng & Li, 2014). Squares of 2 × 2 cm were cut from each film, then weighed to the nearest 0.0001 g on an analytical scale, which was the initial mass (M1). The samples were then dried in an oven at 70 °C for 24 h, and weighed again, which was the initial dry mass (M2). For the next measurement, the samples were placed on sterile Petri dishes in 30 ml of water and kept covered at room temperature. After 24 h, the samples were removed from the water, gently dried with filter paper and weighed again (M3). They were then placed back in the oven at 70 °C and after 24 h the final dry weight was measured (M4.) Three measurements of each value were taken for each film and the mean value of the measurements calculated.

The analysed parameters were calculated according to the formulae:

$$\text{Water content } [\%] = \frac{M_1 - M_2}{M_1} x100$$

$$\text{Solubility } [\%] == \frac{M_2 - M_4}{M_2} x100$$

$$\text{liquid absorption capacity } [\%] == \frac{M_3 - M_2}{M_2} x100$$

2.12. Thickness and transparency

The thickness of films was determined using manual instrument Mitotuyo, No. 7327 (Kawasaki, Japan) The measurements were performed with the 1 μm precision at five random positions on each testing specimen used for WVTR and for physical properties test and two positions for transparency test. The average of film thickness values were used in all calculations.

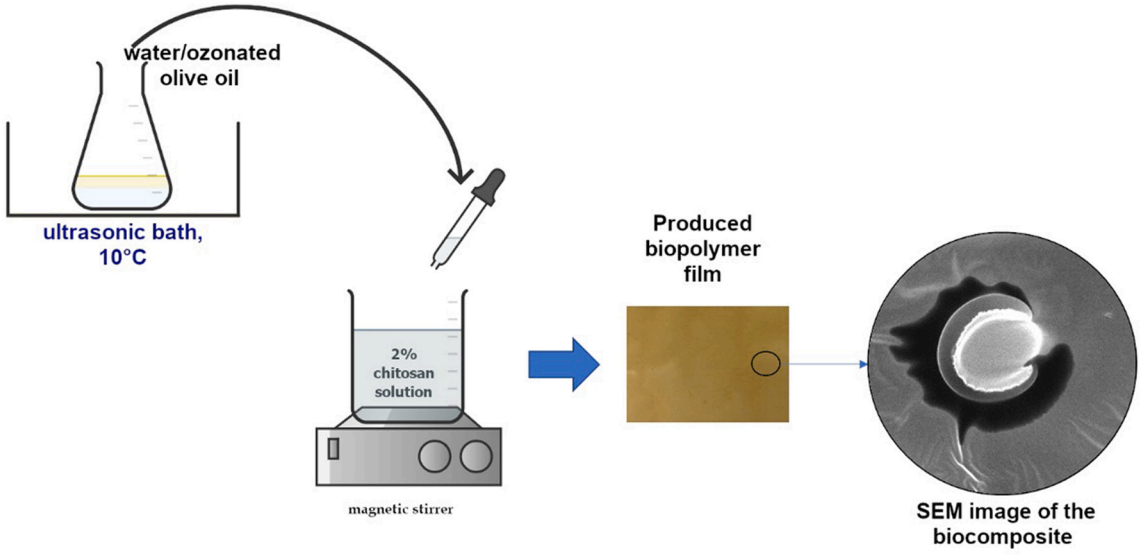

Fig. 1. Schematic diagram of procedure for composite preparation.

Strips of film measuring 30 × 10 mm were cut and analysed in a UV–visible spectrophotometer Shimadzu 2101 (Shimadzu, Kyoto, Japan) scanning. The films were placed directly in the quartz cell for measurement, an empty cuvette was used as a reference. The transparency was determined at 600 nm using a UV–visible spectrophotometer, and was calculated by the equation (Krystyjan et al., 2021):

$$T = A_{600}/x$$

where A_{600} is the absorbance at 600 (nm) and x is the film thickness (mm). A higher value of T indicates a lower degree of transparency.

2.13. Water vapour transmission rate (WVTR)

The glass vessel was filled with silica gel, covered with analysed film and sealed tightly. Then, it was placed in a regulated microclimatic chamber (temperature 25 °C and 75% of relative humidity). After 24 h, the vessel was weighed. The water Vapour Transmission Rate was determined on the basis of weight gain. The test was repeated 5 times for each sample. WVTR was calculated according to the formula:

$$\text{WVTR}\left[g/m^2 \times d\right] = 240 \times \text{weight of water} \div (\text{surface penetration} \times 24)$$

2.14. Contact angle determination

The subsequent study was focussed on determining the contact properties and surface free energy of the foils. These were characterised by defining the dynamic contact angles between the tested foil sample and the polar and non-polar liquids. These analyses were performed using a Krüss DSA100M Drop Shape Analyzer optical contact angle measuring instrument (Gmbh, Hamburg, Germany). Stainless steel syringe needles (NE 44, Krüss Gmbh, Hamburg, Germany) were used for each new analysis. The Krüss DSA100M uses an optical microscope and a digital camera (200 fps) that takes high-speed images of the tested material and uses a digital image processing algorithm to calculate the contact angle of the droplet based on the Young-Laplace equation. During the measurements, the environmental chamber temperature was controlled using a thermostatic water bath, which maintained constant humidity and constant temperature conditions (22.0 ± 0.3 °C). For each tested sample, more than three successive analyses were performed. It means from 6 to 12 successful contact angle measurements with water and the same number of experiments with diiodomethane. We present the average value from tests and the standard deviation in the paper. For diiodomethane we present the equilibrium data of contact angle. Only in the case of water we were forced to use the initial contact angle in the case of water because no real equilibrium could be reached with studied biopolymers as they absorb water and swell. However, the effect of dispersive interaction between the polar solvent (water) and sample is so small that even if it is overestimated (due to the use of the initial contact angle), it still is negligible in the analysis of free surface energy. Thanks to the use of the Krüss DSA100M Drop Shape Analyzer equipped with a digital camera working with high speed of data acquisition, the moment of drop formation was captured with the accuracy of a fraction of a second. To determine this parameter, the Owens–Wendt method (Rudawska & Jacniacka, 2009), which is generally accepted as the best for polymer substances evaluations, was applied. The same methodology was applied for polar and non-polar solvents (i.e., pure water δ = 72.30 mN/m (Millipore Q, 18.60 mΩ/cm), diiodomethane δ = 50.80 mN/m).

2.15. Particle size and zeta potential analysis

The foils were dissolved in distilled water in the presence of 1% acetic acid (due to the presence of chitosan). The mixtures were mixed for 12 h on the magnetic stirrer and evaluated for the particle size dispersion and zeta potential using a Zetasizer Nano Series ZS (Malvern, UK). The measurement were repeated a few times and the average value from all experiments was calculated.

2.16. Enzymatic hydrolysis

Chitosan 2.5 mg (on a dry weight basis) films were placed in 70 ml of 0.1 M acetate buffer, pH 5.5. The mixture was thermostated in a 37 °C water bath for approximately 15 min, and then enzyme solution (1.2 ml) was added. After adding the enzyme, the reaction mixture was incubated with gentle stirring at 37 °C. Samples of the reaction mixture (3.0 ml) were taken after 0, 10, 20, 40, 60, 80, 100, 120, 140, 160, 180, 200 and 220 min for the determination of the reducing sugars. The enzymatic hydrolysis reaction was stopped by adding 3 ml of DNS solution. Samples after the reaction were filtered through 0.2 μm pore diameter cellulose strainers (Waterman) and heated at 90 °C for 5 min and cooled to 20 °C. Then a UV–Vis spectrophotometric analysis was carried out on a Shimadzu TCC-260 spectrophotometer. The absorbance at 520 nm was recorded, and the calibration curve was prepared using D-(+Glucosamine hydrochloride) (Sigma-Aldrich, Poznań, Poland) as standard.

All reactions were run in duplicate.

2.17. Acid hydrolysis

Chitosan 2.5 mg (on a dry weight basis) films were placed in 70 ml of 0.1 M hydrochloric acid. The mixture was thermostated in a water bath at 25 °C. Samples of the reaction mixture (3.0 ml) were taken after 0, 20, 40, 60, 80, 120, 185, 240, 310, 360, 400, 420, 480, 550, 600, 660, 720 min for determination of the concentration of reducing sugars.

The hydrolysis reaction was stopped by adding 3 ml of alkaline DNS solution. 3,5-Dinitrosalicylic acid (DNS) in alkaline sodium potassium tartrate was used as the reagent for reducing sugars according to Southgate (Southgate, D.A.T. AFRC Institute of Food Research, Norwich Laboratory, N. United K, 1991). Samples were filtered through 0.2 μm pore diameter cellulose strainers (Waterman) and assayed for reducing sugars by UV–Vis spectrophotometry from 480 to 520 nm on a Shimadzu TCC-260 spectrophotometer. The calibration curve was prepared using D-(+) Glucosamine hydrochloride (Sigma-Aldrich, Poznań, Poland) as standard.

All reactions were run in duplicate.

2.18. Microbiological analysis

Microbiological testing was performed according to PN-EN ISO 4833-2:2013–12 + AC:2014–04, PN-EN ISO 21528-2:2017–08, PN-EN ISO 6888-2:2001 + A1:2004, PN -EN ISO 11290 -1:2017–07, PN-EN ISO 10272-2:2017–10, and PN-ISO 16649-2:2004. Two replicates were performed for each of the films received. Initially, containers were prepared for each of the analysed samples (K, 0_3–0.5 and 0_3–1) and for the polyethylene stretch foil for food packaging (FS) by placing a piece of analysed, sterilised film in the cap. The films were sterilised by exposing them to ultraviolet light for 30 min. Five pieces of pork weighing 1 g (±0.05 g) were then placed in each container. The material was kept under refrigeration for 4 days, with one piece removed each day for microbiological analysis. The results obtained were statistically analysed using the Turkey test and one-way analysis of variance. The analysis included a comparison of each film sample tested separately for different times (24, 48, 72, 96 h) and microorganisms.

2.19. Photoluminescence spectroscopy (PL)

PL spectra were measured to confirm the optical properties of the produced films and any sensitivity to changes in the environment. PL measurements for the films were carried out at room temperature using a HITACHI F7000 spectrophotometer (Hitachi Co. Ltd., Japan). A wavelength of 360 nm was used for excitation. The emission spectra of

the films were measured before the storage test and after four days of the pork meat being stored under them.

2.20. Statistical analysis

Differences among data mean values were tested for statistical significance at the $p < 0.05$ level using Duncan's multiple range tests and Turkey test. Statistical package for the social sciences SPSS (IBM Corporation) was used for all applied analysis. Data are presented as mean ± SD.

3. Results and discussion

3.1. Scanning electron microscopy

Fig. 2 shows SEM images of the composites obtained. SEM confirmed the desired nanostructures were obtained, which are not observed in the control film. For the O_3_0.5 film (Fig. 2 D, E and F), we observe the formation of nanostructures with a narrow capsule size distribution in the range of 800–1000 nm, while for the O_3–1.0 film (Fig. 2 G, H and I), we observe a relatively wide capsule size distribution (from 1000 nm to 1500 nm) at the same time aggregates. During the analysis, under the influence of the electron beam, destruction of the nanocapsule structure was observed, which is illustrated by Fig. 2 E for the O_3_0.5 composite and H for the O_3_1.0 composite. Fig. 2 I shows single nanocapsules with a characteristic core-shell arrangement.

3.2. UV–Vis spectrophotometry

Fig. 3 shows the UV–Vis absorption spectra of the obtained films. The bands at 380–460 nm of wavelength indicate that the composite absorbs light in the blue and near ultraviolet range, which is characteristic of chitosan composites(Aziz & Hazrin Abidin, 2014). The addition of nanocapsules of ozonated olive oil at the higher concentration (O_3_1.0) caused the composite to absorb visible and ultraviolet light to a greater extent. In the literature (Rajabi, Shamsipur, Khosravi, Khani, & Yousefi, 2013), the relationship between the size of nanoparticles and their UV–Vis spectrum is well known. The results presented here show that the size of the nanoparticles obtained varies, which coincides with the SEM and DLS results.

3.3. FTIR-ATR spectroscopy

Performing a FTIR analysis made it possible to analyse the chemical

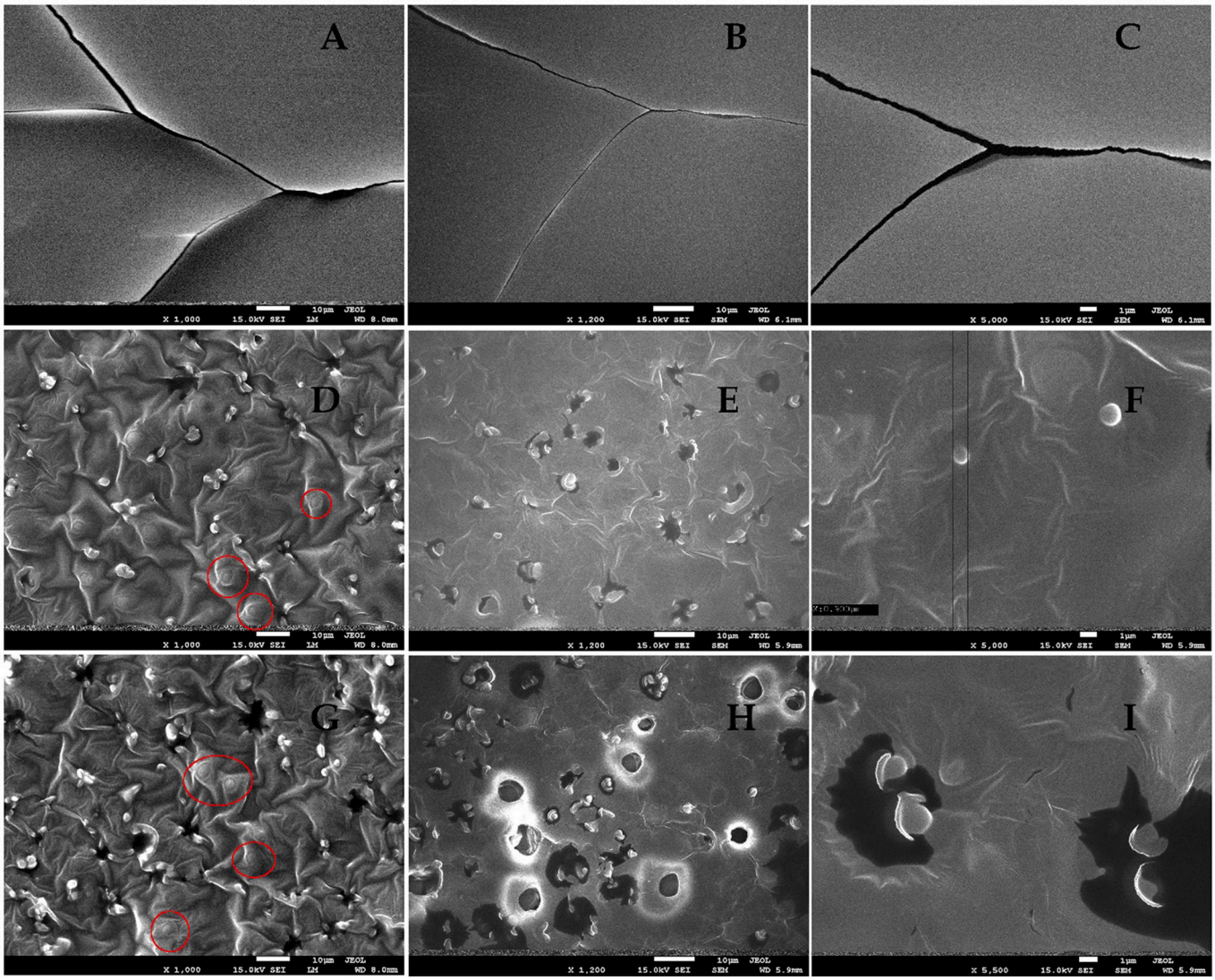

Fig. 2. SEM image of the biocomposites: A, B and C – for control sample (K) at magnification of x1000, x1200 and x5000, respectively; D, E, F – for composite O_3_0.5 at magnifications of x1000, x1200 and x5000, respectively; G, H and I – for composite O_3_1.0 at magnifications of x1000, x1200 and x5500, respectively.

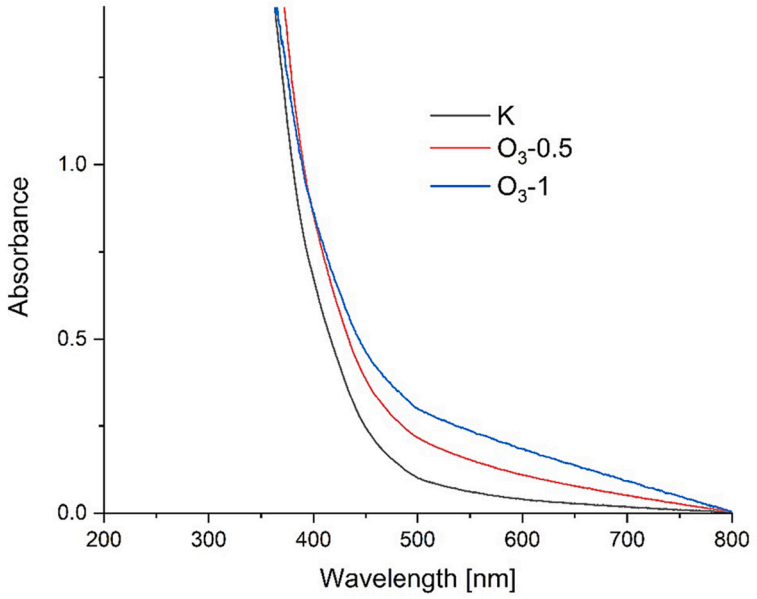

Fig. 3. UV–Vis spectra of control film (K), and those containing nanocapsules of ozonated olive oil at two concentrations (O_3_0.5 and O_3_1.0).

structure of the composites obtained. The obtained spectra shown in Fig. 4 are characteristic of the spectrum of chitosan (Baroudi, García-Payo, & Khayet, 2018). The addition of ozonated olive oil nanocapsules did not significantly affect the structural changes of the polymer, which proves that chitosan is a good matrix for the formation of ozonated olive oil nanocapsules. The typical band corresponding to the structure of chitosan is in the range 932–1125 cm^{-1} and corresponds to C-O-C bonds, the vibrations at 1414 cm^{-1} are characteristic of C—H groups, while at 1544 of NH_2 amino groups. The vibrations at the wave number 1633 cm^{-1} are characteristic of C═O amide groups, and here we observe a shift in the spectra for the samples containing ozonated olive oil compared to the control film. Similarly, in the 1800–1700 cm^{-1} range, we observe a peak only for samples containing ozonated olive oil nanocapsules, which correspond to the C═O groups of oil. The range 2961–2340 cm^{-1} corresponds to the CH_2 groups. -OH hydrogen groups are responsible for the oscillations of the 3622–2986 cm^{-1} range (Krystyjan et al., 2021; Sadowska et al., 2008; Wang et al., 2017).

3.4. Optical properties

In order to determine the optical properties, the composites obtained were subjected to a simple optical test. Using a lamp, they were exposed to UV light and the fluorescence of all three samples was observed (Fig. 5). All samples show blue fluorescence, which results from the emission properties of chitosan (Hm, Mh, Yi, & Wh, 2017).

3.5. Determination of water content, solubility and liquid absorption capacity

The water content, solubility and liquid absorption capacity are

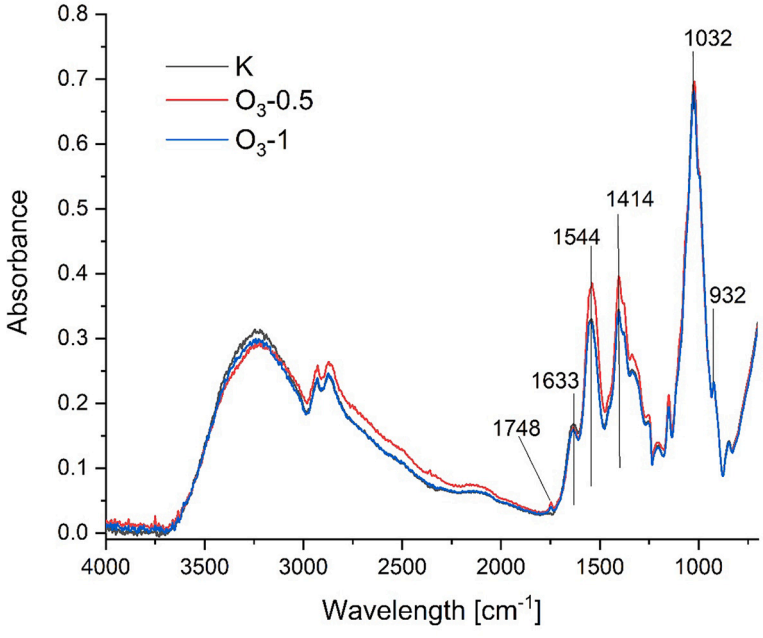

Fig. 4. FTIR-ATR spectra of the composites obtained.

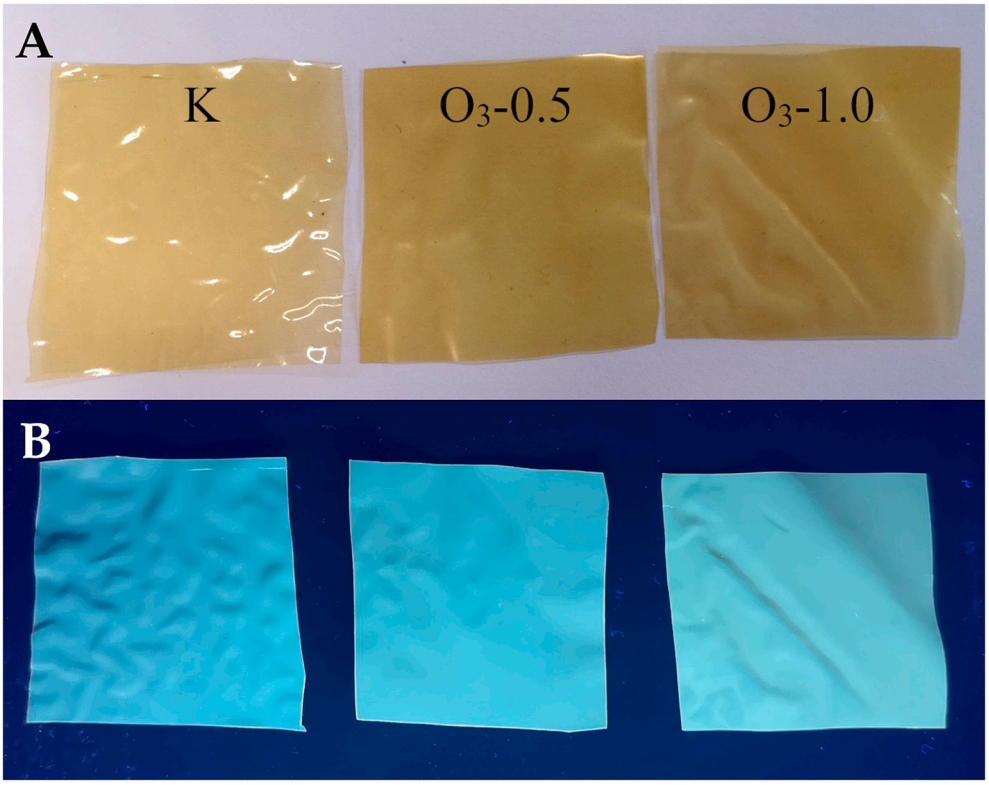

Fig. 5. Produced biopolymer films A – in daylight, and B – in the dark under UV light.

presented in Table 1. The results obtained show that the addition of ozonated olive oil directly affects the parameters determined, and the effect depends on the amount of oil. Lipid compounds improve the water barrier properties of polymer-based films due to their hydrophilic nature. The film containing the highest concentration of ozonated olive oil (O_3_1.0) has the lowest water content. The control film (K) is more than twice as high, while the film with the lower concentration of ozonated olive oil (O_3_0.5) was between them (water content of 14.01%). The addition of nanocapsules of ozonated olive oil resulted in the breaking of hydrogen bonds between chitosan and water, and consequently a lower water content. It also affected the solubility and liquid absorption capacity which decreased by 10.39% and 30.01%, respectively, compared to the control film. The changes in solubility values and liquid absorption capacity are related to water diffusion, dissociation of hydrogen and ionic bonds, ionisation of carboxyl or amino groups and relaxation of the polymer (Mathew, Brahmakumar, & Abraham, 2006; Peng & Li, 2014; Sánchez-González, Vargas, González-Martínez, Chiralt, & Cháfer, 2009).

In the O_3–0.5 film, there was an interaction between the oil and the chitosan, thus reducing the solubility of the composite. The increase in solubility after the addition of a higher concentration of ozonated olive oil is possibly related to the leaching of ozonated olive oil nanocapsules not bound to the polymer from the polysaccharide surface, which as visualised by SEM microscopy is characterised by a porous structure.

3.6. Thickness and transparency

Thickness and transparency of the films are shown in Table 1. The thickness of the chitosan film was the highest and was significantly ($P < 0.05$) different from the capsule film. The addition of ozonated olive oil capsules significantly reduced film thickness and water content at the same time. Park et al. (Park, Weller, Vergano, & Testin, 1993) attributed the effect on thickness to changes in film structure resulting from water content and liquid absorption capacity in the biopolymer (Ortiz-Duarte, Martínez-Hernández, Casillas-Peñuelas, & Pérez-Cabrera, 2021). The film thickness ranged from 0.038 to 0.053 mm, similar to other natural biopolymer films and met the definition of film <0.25 mm (Giteru et al., 2015).

As Hutchings (Hutchings, 1999) has shown, the most relevant properties when evaluating the effect on color and appearance of a coated product are transparency, opacity and brightness. It is worth mentioning that higher value of T indicates lower transparency and high degree of opacity.

In this study, the transparency of chitosan-based films was significantly ($P < 0.05$) higher than those containing ozonated olive oil capsules, and the addition of olive oil significantly reduced the transparency from 0.24 to 4.11. This difference may be due to the color of the films. The films containing ozonated allium capsules were darker (Fig. 4) therefore their transparency was lower (Ortiz-Duarte et al., 2021). The addition of ozonated olive oil reduced the transparency of the film, which may have preventing effect on photodegradation of the material when light is transmitted during storage periods (Sanuja, Agalya, & Umapathy, 2015).

3.7. Water vapour barrier properties

The highest water vapour barrier properties were found for chitosan-based films. This is most likely due to the natural hydrophilicity of chitosan. The WVTR decreases significantly with increase in the amount of addition of capsulated olive oil by 4.53% for film containing lower concentration and by 13% for film containing higher concentration of ozonated olive oil. The observed phenomenon is due to the hydrophobic nature of olive oil. Thus, the film masks the path of water vapour penetration into the material which affects the stability of the film and the ability to prevent the onset of microbial degradation of stored food (Saral Sarojini, Indumathi, & Rajarajeswari, 2019; Sanuja et al., 2015).

Table 1
Thickness, water content, solubility, liquid absorption capacity, Water Vapour Transmission Rate and transparency of the composites obtained.

Sample	Thickness (mm)	Water content (%)	Solubility (%)	Liquid absorption capacity (%)	WVTR (g/m2·d)	T ($A \cdot mm^{-1}$)
K	0.053^{a}	$16.4^{a} \pm 0.43$	$7.02^{a} \pm 0.92$	$59.40^{a} \pm 2.25$	$113.76^{a} \pm 3.31$	$0.24^{a} \pm 0.07$
O_3–0.5	0.044^{b}	$14.01^{b} \pm 0.61$	$4.53^{b} \pm 0.28$	$49.01^{a} \pm 1.50$	$109.23^{b} \pm 3.30$	$2.88^{b} \pm 0.35$
O_3–1	0.038^{b}	$7.2^{c} \pm 0.54$	$11.47^{c} \pm 0.82$	$29.39^{b} \pm 1.51$	$100.69^{c} \pm 1.32$	$4.11^{c} \pm 0.59$

Parameters in columns denoted with the same letters (a. b. c.) do not differ statistically at the confidence level of $p < 0.05$.

3.8. Particle size and zeta potential analysis

Particle and aggregate sizes were measured after dissolving film samples of the same masses in 1% acetic acid. We observe aggregates with sizes of 300–800 nm in the samples and probably sedimenting particles with sizes exceeding 3500 nm and reaching 5000 nm. Samples from the control film have the highest polydispersity of smaller aggregates, from 300 down to 60 nm, and the smallest particles with sizes on the order of 3500 nm. Particles from the film containing O_3_0.5, on the other hand, have the largest recorded aggregates with sizes of 800 nm and particles with sizes of 4900 nm. In the case of the film containing the maximum O_3 saturation, we see a broad Gaussian peak on the DLS spectrum showing aggregates with sizes from 100 to 1000 nm, with a predominance of fractions of 300–400 nm. We also observe here a small peak from particles with sizes of 5500 nm.

The zeta potential measurements carried out show a gradual increase of the potential with increasing the proportion of O_3 saturation in the films studied. Particles from control films show zeta potentials of 26 mV, while for the O_3–0.5 and O_3_1.0 particles, values of 32 mV (O_3_0.5) and 52 mV (O_3_1.0) were measured.

3.9. Contact angles

All tested samples show high hydrophobicity, which is proven by the contact angles for water in the range 85–88° and contact angles for diiodomethane in the range of 40°. The performed measurements prove that the hydrophobicity of the samples slightly decreases with an increase in O_3 content. The surface energies calculated on the basis of contact angle measurements prove that dispersive surface free energy predominates in the samples. The polar component of the surface energy is practically negligible. However, the values of the dispersive energy decrease slightly with the increasing O_3 content, while the polar component of the surface energy increases slightly (Table 2).

3.10. Enzymatic hydrolysis

Fig. 6 shows the dependence of the concentration of reducing sugars per glucosamine on the reaction time of the enzymatic hydrolysis of chitosan films.

In Fig. 7, using linear regression and the relation of log(1/c) to time, t, rate constants for the subsequent stage of the enzymatic reaction were calculated from the correlation of linear regression $R = 0.97–0.99$. The reaction appeared to be the first order process (Table 3). The rate constants *(k)* of the enzymatic hydrolysis reaction were determined as the slope coefficient of the straight line (Fig. 7), the values of the rate constants are presented in Table 3.

Fig. 8 shows the dependence of the concentration of reducing sugars per glucosamine on the reaction time of the acid hydrolysis of the chitosan films.

The acid hydrolysis of the chitosan films proceeds in two steps having a linear dependence of product growth on reaction time. This course of degradation is suggested by the zero order of the acid hydrolysis reaction of the chitosan films. For each of the linear stages of the hydrolysis reaction, reaction rate constants *(k)* were determined as the slope coefficient of the straight line. The values of the rate constants *(k)* are presented in Table 3.

For all three films, the enzymatic hydrolysis reaction yields after 80 and 220 min and the acid hydrolysis yields after 80 and 720 min were determined (Table 4).

The linear dependence of log(1/c) on the hydrolysis time indicates that the enzymatic hydrolysis of the films is a first order reaction. The values of rate constants show that the fastest hydrolysis is for the O_3_0.5 film containing 0.5 ozonated oil, followed by the control K film without ozonated oil, and the slowest enzymatic hydrolysis was for the O_3_1.0 film.

The acid hydrolysis of the chitosan films proceeds in two steps having a linear dependence of product growth on reaction time. This course of degradation is suggested by the zero order of the acid hydrolysis reaction of the chitosan films. The values of rate constants show that similarly as in the case of enzymatic hydrolysis, the fastest hydrolysis was observed for the O_3_0.5 film containing 0.5 ozonated oil, then for the control K film without ozonated oil, while the slowest enzymatic hydrolysis was observed for the O_3_1.0 film.

3.11. Microbiological analysis

The study of the antimicrobial properties of the composites obtained included the evaluation of the microbiological quality of pork meat stored under the manufactured films at +4 °C. Figs. 9–13 show the results from microbiological cultures for individual groups and species of bacteria as a function of time (24 h, 48 h, 72 h, 96 h). The following were analysed: total number of microorganisms (Fig. 9), number of coagulase-positive staphylococci (Fig. 10), number of *Enterobacteriaceae* bacteria (Fig. 11), number of *Escherichia coli* bacteria (Fig. 12), number of *Campylobacter* spp. bacteria (Fig. 13) and *Listeria Monocytogenes*, the presence of which was not detected in either the fresh or stored meat (not included in the graph), so the effect of the composites analysed on this bacterium cannot be assessed.

No *Escherichia Coli* or *Campylobacter* spp. were detected in fresh meat (O h of incubation). The total number of microorganisms was 86 CFU/cm^3, 3 colonies of *Enterobacteriaceae* and 103 colonies of coagulase-positive staphylococci were detected. The lowest microbiological quality was characterised by pork meat stored under food film. The foil did not show any antimicrobial effect and the number of microorganisms determined increased continuously during the following days. The results obtained indicate a strong effect of the composites on the total number of microorganisms in the pork meat. Comparing the data from the last, 4th day of storage, the total number of microorganisms for the food film was 279 CFU/cm^3, while for O_3_1.0 only 173. This value is almost half as high, which confirms the literature data and general state of knowledge that both chitosan and ozone show bactericidal and bacteriostatic properties.

The mechanism of bactericidal effect of chitosan has been extensively studied for several years (Kong, Chen, Xing, & Park, 2010; Kumirska, Weinhold, Thöming, & Stepnowski, 2011; Qin, Li, & Guo, 2020; Wu, Long, Xiao, & Dong, 2016) and research hypotheses state that it may be due to the polycationic nature of the polymer – the positive charge of the protonated amino group of chitosan interacts with positively charged molecules on the surface of bacterial cells, causing leakage of intracellular substances and, consequently, bacterial cell death (Chung & Chen, 2008; Costa, Silva, Pina, Tavaria, & Pintado, 2012; H. Liu, Du, Wang, & Sun, 2004). Some findings suggest that

Table 2
Contact angles for water and diiodomethane and calculated values of polar, dispersive and total surface energies according to Owens-Wendt model.

Sample	Contact angle Water	Contact angle Diiodomethane	Polar Surface Energy (mJ/m^2)	Dispersive Surface Energy (mJ/m^2)	Total Surface Free Energy (mJ/m^2)
K	87.53° ± 0.42	47.50° ± 0.31	1.65	38.14	39.78
O_3_0.5	86.13° ± 0.63	43.00° ± 0.25	1.60	40.90	42.50
O_3_1.0	85.45° ± 0.14	36.87° ± 0.09	1.28	44.79	46.06

chitosan may affect the expression of bacterial cell DNA through binding to nucleic acid, which occurs as a result of chitosan penetrating inside the bacterial cell (Galván Márquez et al., 2013; J. Li & Zhuang, 2020; Park, Nah, & Park, 2011). The mechanism of chitosan's bactericidal action depends on many external factors including: chitosan particle size, pH, temperature, bacterial growth phase, type of bacteria, and chitosan concentration. Liu et al. (N. Liu et al., 2006) have shown that the concentration of chitosan is analogous to its antimicrobial effect, and at concentrations above 200 ppm the action is inhibitory which correlates with the results obtained.

The mechanism of bactericidal and bacteriostatic effect of ozone is related to its chemical activity. It reacts with unsaturated aromatic and aliphatic compounds, oxidising them by cyclic addition to the double bonds. Inactivation is related to the oxidation of thiol groups, which are commonly found in microbial enzymes. Ozone reacts slowly with polysaccharides, leading to the formation of aliphatic acids and aldehydes by breaking glycosidic bonds. Reaction with primary and secondary aliphatic alcohols can lead to hydroxyhydroperoxides, which are precursors of hydroxyl radicals. These in turn react strongly with hydrocarbons(Giuliani, Ricevuti, Galoforo, & Franzini, 2018).

As shown by Rey et al. (Rey, Núñez Sellés, Baluja, & Lorenzo Otero, 2008), *N*-acetylglucosamine present in the cell walls of Gram-positive and Gram-negative bacteria is resistant to ozone in the pH range 2–7. Gram-positive bacteria have a higher content of this peptidoglycan in

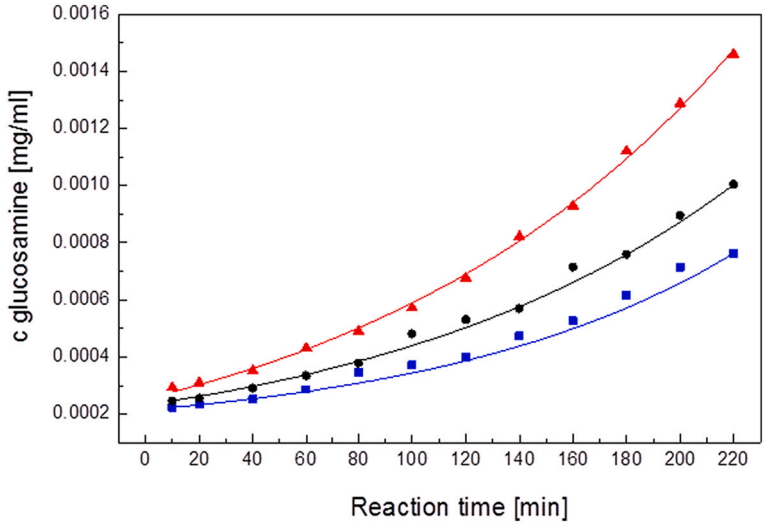

Fig. 6. Dependence of the concentration of reducing sugars per glucosamine on the enzymatic hydrolysis reaction time for films: —— K, —— O_3_0.5, —— O_3_1.0.

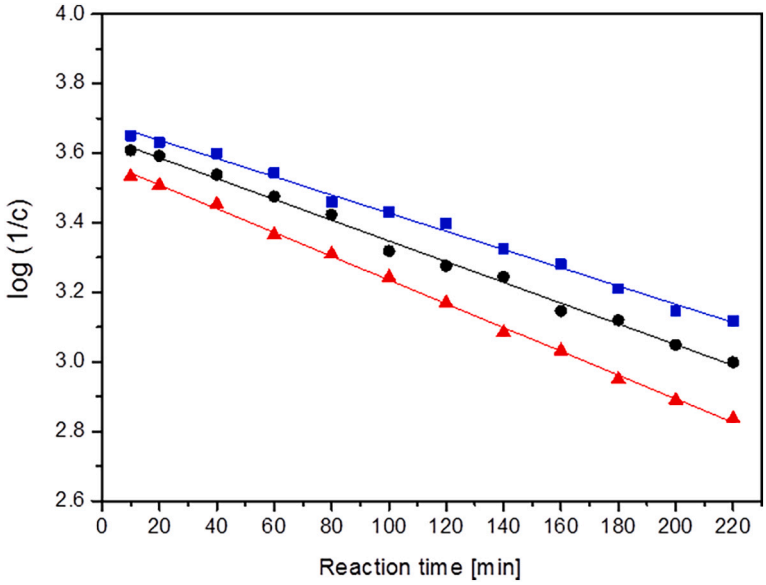

Fig. 7. Dependence of log (1/c) on the reaction time of enzymatic hydrolysis of chitosan films: —— K, —— O_3_0.5, —— O_3_1.0.

Table 3
Rate constants of the enzymatic hydrolysis and acid hydrolysis of the chitosan films.

Hydrolysis	Rate constant		
	enzymatic	acid	
	k x 10^{-3} [min^{-1}]	k_1 x 10^{-6} [$mg \bullet ml^{-1} \bullet min^{-1}$]	k_2 x 10^{-6} [$mg \bullet ml^{-1} \bullet min^{-1}$]
O_3_0.5	3.42 ± 0.03	6.7 ± 0.02	1.05 ± 0.02
O_3_1.0	2.62 ± 0.02	2.7 ± 0.01	0.82 ± 0.02
K	2.99 ± 0.03	3.6 ± 0.02	0.93 ± 0.03

their cell wall composition compared to Gram-negative bacteria. This seems to explain the inferior bactericidal and bacteriostatic effect of ozone against Gram-positive bacteria, which include among others *Staphylococcus Aureus*, compared to e.g. *Escherichi Coli*, which was also analysed. In the obtained results, we observe inhibition of *Staphylococcus aureus* growth for the K, O_3–0.5 and O_3–1.0 films in comparison with the food films in the last day of storage. The addition of ozone to the film did not increase the antimicrobial activity, which is based solely on the effect of the chitosan. In contrast to the results obtained for *Staphylococcus aureus*, in the case of the analysed Gram-negative bacteria, i.e. *Enterobacteriaceae* and *Escherichia Coli*, the addition of nanocapsules of ozonated olive oil increased the antimicrobial effect of the composite. In the literature, there are many descriptions of using chitosan-based films for extending food storage times (Rodríguez-Rojas, Arango Ospina, Rodríguez-Vélez, & Arana-Florez, 2019). These properties were enhanced by placing natural antimicrobial agents in the film, such as essential oils (Valizadeh, Naseri, Babaei, Hosseini, & Imani, 2019; Xu et al., 2019) or antimicrobial agents based on metal nanostructures and metal oxides, such as silver or copper nanoparticles, with promising results (Kumar, Mukherjee, & Dutta, 2020). Contrary to nanometals, the use of essential oils allows for the production of a completely natural, biodegradable and environmentally-friendly film, but it does not always improve the antimicrobial effect. According to Gómez-Estaca et al. (Gómez-Estaca, López de Lacey, López-Caballero, Gómez-Guillén, & Montero, 2010) in the case of *Escherichia Coli*, only using clove essential oil allowed a complete microbial growth inhibition, while for pine or cypress essential oil no zone of microbial growth inhibition was observed. These limitations, as well as the fact that essential oils can affect the taste and aroma of food products (Siripatrawan, 2016) due to their strong smell, lead to the search for alternative additives to chitosan films. Ozonated oils show strong bactericidal properties against *S. aureus* or *Escherichia coli* (Sechi et al., 2001; Serio et al., 2017; Ugazio et al., 2020), and their use with bactericidal chitosan allows to enhance its properties, which was observed in the above results.

The presence of significant differences in the zone of microbial growth inhibition for the Enterobacteriaceae on the 3rd day of storage may be related to the slow release of the ozone encapsulated in the nanocapsules. The observed zones of inhibition of *Campylobacter* spp. growth do not significantly differ between the analysed films. The sensitivity of *Campylobacter* spp. to chitosan depends on many factors, including: bacterial strain, growth phase, and temperature (Ganan, Carrascosa, & Martínez-Rodríguez, 2009). According to Olaimat et al. (Olaimat, Fang, & Holley, 2014)the sensitivity of *Campylobacter* spp. to chitosan decreases significantly at 4 degrees. The analysed samples were stored in refrigerated conditions, which may explain the lack of a significant zone of growth inhibition.

However, due to the visible mechanism of antibacterial activity of nanocapsules of ozonated olive oil on this bacterium, the study will be continued.

The use of ozone in meat industry or as an additive to active packaging may be questionable due to its strong oxidising properties, which may deteriorate the final quality parameters of the product. The degradation of the color parameter occurs as a result of the oxidation of myoglobin and oxymyoglobin and, consequently, the development of metamioglobin, which reduces the redness of the meat and affects negatively the consumer's perception of the product. Ozone, as a reactive form of oxygen, can also contribute to lipid oxidation (Muhlisin, Utama, Lee, Choi, & Lee, 2016). However, it has been shown that there is a direct relationship between the time of ozonization and its concentration, and adjusting the appropriate parameters allows to maintain the antimicrobial effect while maintaining an appropriate color parameter and controlling lipid oxidation (Coll Cárdenas, Andrés, Giannuzzi, & Zaritzky, 2011). Moreover, as demonstrated by Piachin and Trachoo, combining the ozonation process with the use of other compounds, such as potassium lactate or carbon monoxide, allows better color stabilization during storage compared to untreated samples, while improving the microbiological quality and reducing the oxidation of fats (Piachin & Trachoo, 2011). Calcium lactate contributes to the maintenance of the color value by increasing the activity of lactic acid hydrogenase, which in turn promotes the activity of metmyoglobin producing oxymyoglobin or deoxymyoglobin. Currently chlorine is widely used as a disinfectant in the processing of meat. Comparing poultry meat treated with chlorine with poultry meat treated with ozone did not show any significant differences in sensory characteristics, which favors the possibility of using

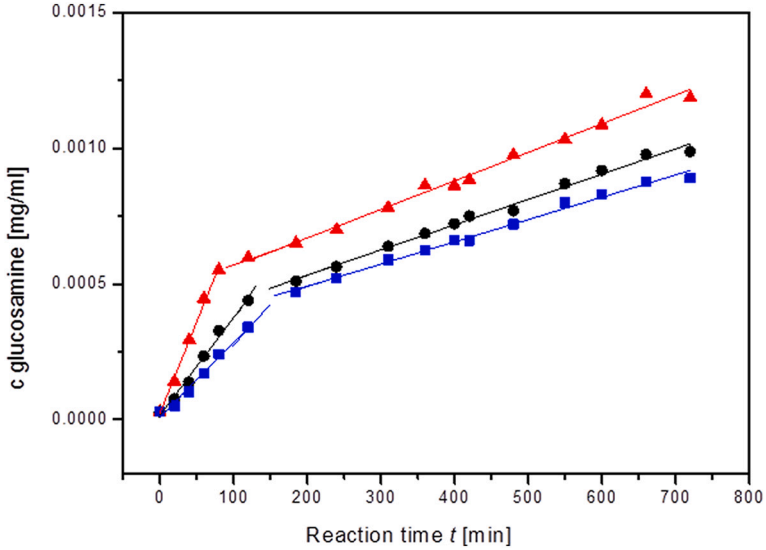

Fig. 8. Dependence of the concentration of reducing sugars per glucosamine on the acid hydrolysis reaction time for films: —— K, —— O_3_0.5, —— O_3_1.0.

Table 4
Efficiency of enzymatic and acid hydrolysis reactions for the chitosan films.

Hydrolysis	Yield of the hydrolysis reaction after time			
	enzymatic		acid	
	80 min	220 min	80 min	720 min
	x 10^{-4} [mg•ml^{-1}]	x 10^{-4} [mg•ml^{-1}]	x 10^{-4} [mg•ml^{-1}]	x 10^{-4} [mg•ml^{-1}]
O_3_0.5	3.8	14.6	5.5	11.9
O_3_1.0	3.4	7.6	2.4	8.9
K	3.5	10.0	3.4	9.9

ozone in the meat industry (Khanashyam, Shanker, Kothakota, Mahanti, & Pandiselvam, 2021; Stivarius, Pohlman, McElyea, & Apple, 2002), however, the use of ozone in such a packaging system will be subject to further investigation.

3.12. Photoluminescence spectroscopy

Fig. 14 show the emission spectra of the composites before storage (red line) and after 4 days of storage of pork meat samples under them (black line).

Fig. 14A shows the emission spectrum of the control film. The chitosan-based composite showed significant light emission at around 440 nm. After 4 days of storage, the emission intensity of the chitosan film decreased significantly. This may be due to relaxation of the polymer and loosening of its structure as a result of absorption of the emitted water from the pork meat. In the conducted analysis of the liquid absorption capacity, the highest value was shown for the control film.

Fig. 14B and C show the emission spectra of chitosan-based films containing nanocapsules of ozonated olive oil. In both cases, the film before storage of pork meat showed significant light emission at around 440 nm, similar to the control film (Fig. 14A). The addition of ozonated olive oil nanocapsules significantly enhances the photoluminescence of the composite and depends on its concentration. The higher concentration of ozonated olive oil nanocapsules doubled the fluorescence intensity of the composite.

A significant decrease in emission values was observed in all films. This may be due to the sensitivity of the composites to the physicochemical and biochemical transformation products formed as a result of meat spoilage.

4. Conclusions

An innovative and environmentally non-toxic chitosan-based biopolymer film was successfully developed and nanocapsules of ozonated olive oil were generated within it. There was no significant interaction between the chitosan and the nanocapsules of ozonated olive oil. The results of enzymatic hydrolysis and acid hydrolysis of the chitosan films indicate that the O_3_0.5 film hydrolysed the fastest, followed

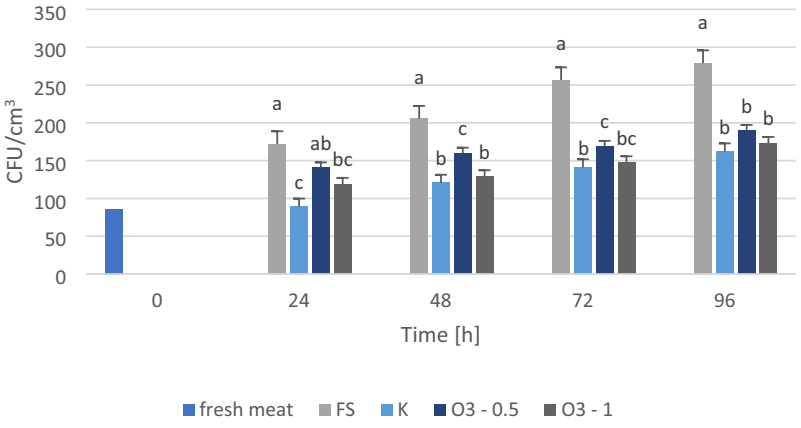

Fig. 9. Total number of microorganisms in pork meat stored at 4 °C under different films. The parameters in columns marked with the same letters (a, b, c, etc.) do not differ statistically at the confidence level of $p < 0.05$.

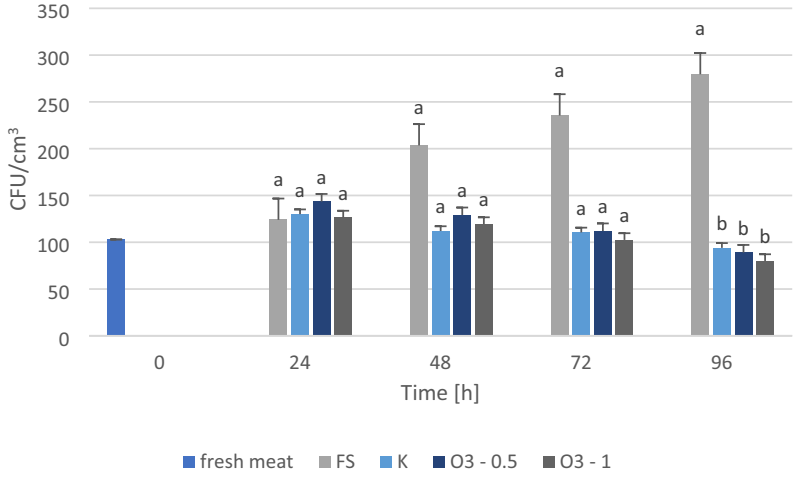

Fig. 10. Number of coagulase-positive staphylococci in pork meat stored at 4 °C under different films. The parameters in columns marked with the same letters (a, b, c, etc.) do not differ statistically at the confidence level of $p < 0.05$.

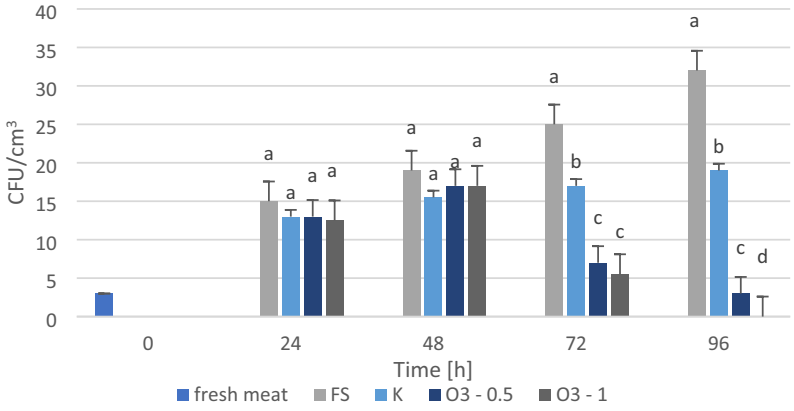

Fig. 11. Number of *Enterobacteriaceae* in pork meat stored at 4 °C under different films. Parameters in columns marked with the same letters (a, b, c, etc.) do not differ statistically at a confidence level of $p < 0.05$.

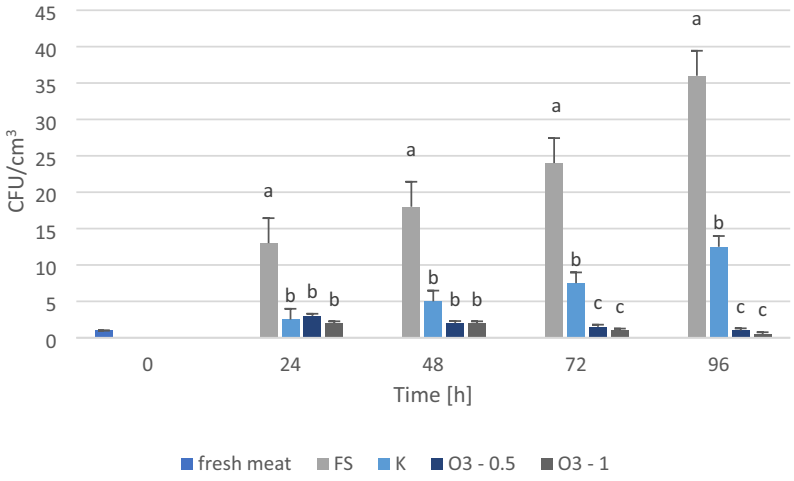

Fig. 12. Number of *Escherichia coli* in pork meat stored at 4 °C under different films. The parameters in columns marked with the same letters (a, b, c, etc.) do not differ statistically at the confidence level of $p < 0.05$.

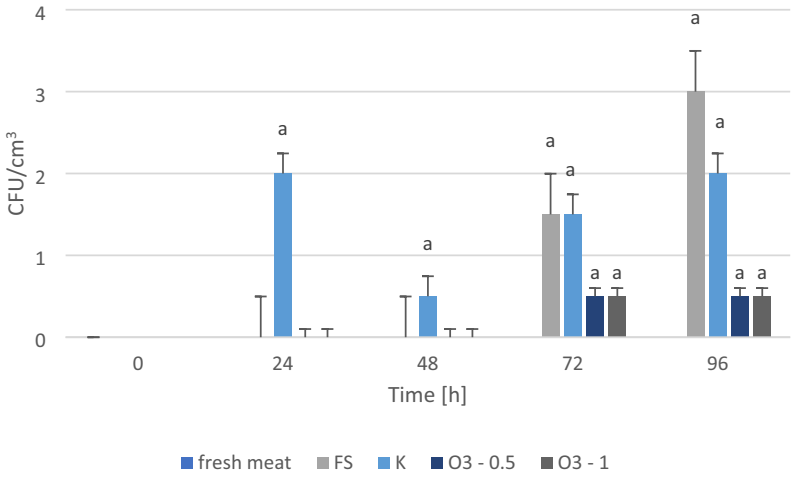

Fig. 13. Number of *Campylobacter* spp. in pork meat stored at 4 °C under different films. The parameters in columns marked with the same letters (a, b, c, etc.) do not differ statistically at the confidence level of $p < 0.05$.

by the control K film, and the progress of enzymatic hydrolysis of the O_3–1.0 film was the slowest. The film susceptibility to enzymatic and acid hydrolysis proves its relatively high biodegradability. These results correlate with the data obtained from the DLS and SEM analyses. The largest particle size was found in the O_3–0.5 film, where sizes up to 4900 nm were observed, in the control film 3500 nm, and in the O_3–1.0 film the predominant fraction had a size of 100–1000 nm. The addition of ozonized olive oil capsules reduced the Water Vapour Transmission

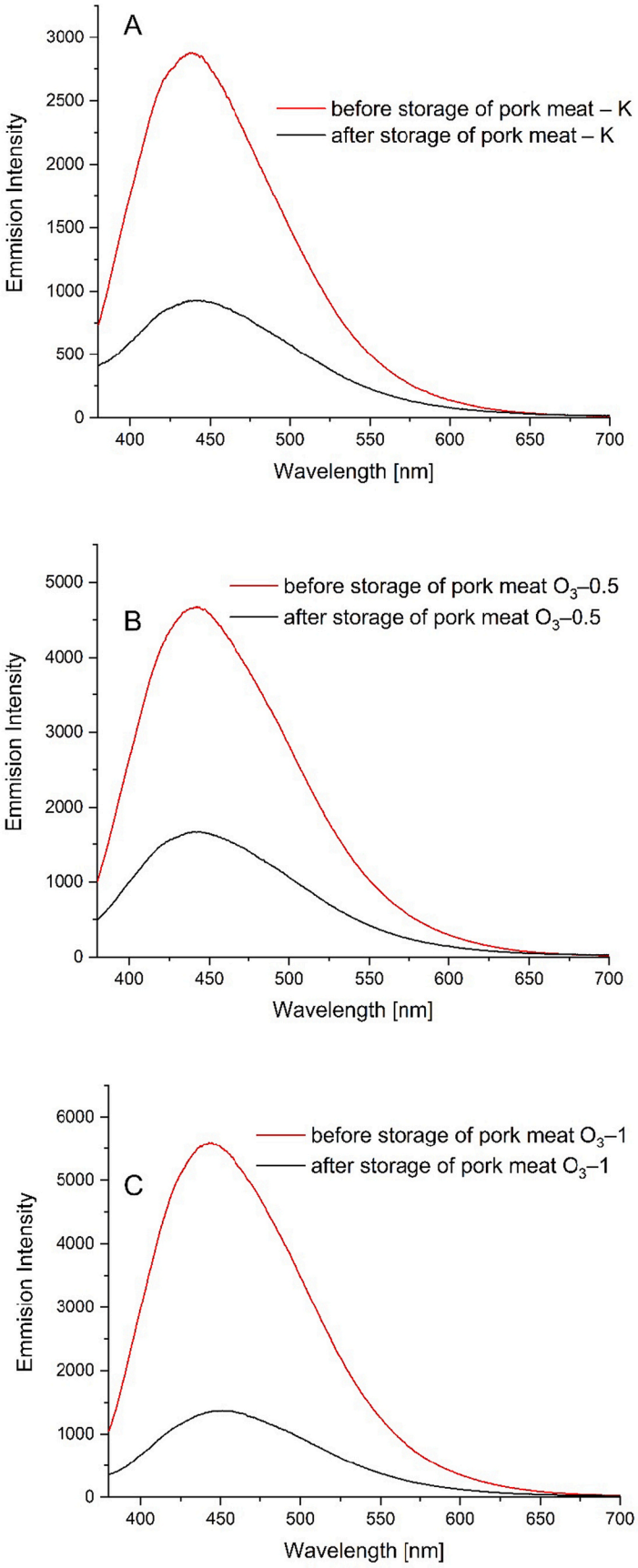

Fig. 14. Emission spectra of control film K (A), O_3_0.5 film (B) and O_3_1.0 film (C) before storage of pork meat (red line) and after 4 days of storage (black line). (For interpretation of the references to color in this figure legend, the reader is referred to the web version of this article.)

Rate and transparency of the film. The microbiological analysis conducted showed that the produced composite had bactericidal and bacteriostatic properties. A decrease in emission values due to spoilage was observed for all of the films, and the generation of nanocapsules of ozonated olive oil significantly enhanced the photoluminescence of the composite. The study conducted showed that the composite can successfully act as a food packaging or packaging element, which extends the shelf life of products while remaining an environmentally neutral alternative to plastic packaging.

Funding

This research was funded by the National Science Centre of Poland, grant no. 2016/21/B/ST8/02107 to M. Krzan and by a subsidy of the Ministry of Science and Higher Education for the University of Agriculture in Krakow for 2021.

CRediT authorship contribution statement

Nikola Nowak: Methodology, Writing – original draft. **Wiktoria Grzebieniarz:** Formal analysis, Validation, Visualization. **Gohar Khachatryan:** Conceptualization, Investigation, Methodology, Writing – original draft, Supervision, Writing – review & editing. **Anna Konieczna-Molenda:** Methodology, Visualization, Writing – original draft. **Marcel Krzan:** Methodology, Writing – original draft. **Karen Khachatryan:** Investigation, Methodology, Supervision, Visualization, Writing – review & editing.

Conflict of interest

None.

References

Adeyeye, O. A., Sadiku, E. R., Babu Reddy, A., Ndamase, A. S., Makgatho, G., Sellamuthu, P. S., … Jamiru, T. (2019). *The use of biopolymers in food packaging* (pp. 137–158). https://doi.org/10.1007/978-981-13-8063-1_6

Almasi, L., Radi, M., Amiri, S., & McClements, D. J. (2021). Fabrication and characterization of antimicrobial biopolymer films containing essential oil-loaded microemulsions or nanoemulsions. *Food Hydrocolloids, 117*, Article 106733. https://doi.org/10.1016/J.FOODHYD.2021.106733

Amjadi, S., Almasi, H., Ghorbani, M., & Ramazani, S. (2020). Reinforced ZnONPs/rosemary essential oil-incorporated zein electrospun nanofibers by κ-carrageenan. *Carbohydrate Polymers, 232*, Article 115800. https://doi.org/10.1016/J.CARBPOL.2019.115800

Amjadi, S., Emaminia, S., Heyat Davudian, S., Pourmohammad, S., Hamishehkar, H., & Roufegarinejad, L. (2019). Preparation and characterization of gelatin-based nanocomposite containing chitosan nanofiber and ZnO nanoparticles. *Carbohydrate Polymers, 216*, 376–384. https://doi.org/10.1016/J.CARBPOL.2019.03.062

Arora, A., & Padua, G. W. (2010). Review: Nanocomposites in food packaging. *Journal of Food Science, 75*(1), R43–R49. https://doi.org/10.1111/J.1750-3841.2009.01456.X

Atarés, L., & Chiralt, A. (2016). Essential oils as additives in biodegradable films and coatings for active food packaging. *Trends in Food Science & Technology, 48*, 51–62. https://doi.org/10.1016/J.TIFS.2015.12.001

Aziz, S. B., & Hazrin Abidin, Z. Z. (2014). *Role of hard-acid/Hard-Base interaction on structural and dielectric behavior of solid polymer electrolytes based on chitosan-XCF 3 SO*. https://doi.org/10.1155/2014/906780

Bahrami, A., Delshadi, R., Assadpour, E., Jafari, S. M., & Williams, L. (2020). Antimicrobial-loaded nanocarriers for food packaging applications. *Advances in Colloid and Interface Science, 278*, Article 102140. https://doi.org/10.1016/J.CIS.2020.102140

Baroudi, A., García-Payo, C., & Khayet, M. (2018). Structural, mechanical, and transport properties of electron beam-irradiated chitosan membranes at different doses. *Polymers, 10*(2), 117. https://doi.org/10.3390/POLYM10020117

Bayarri, B., Cruz-Alcalde, A., López-Vinent, N., Micó, M. M., & Sans, C. (2021). Can ozone inactivate SARS-CoV-2? A review of mechanisms and performance on viruses. *Journal of Hazardous Materials, 415*, Article 125658. https://doi.org/10.1016/J.JHAZMAT.2021.125658

Bilal, M., & Iqbal, H. M. N. (2019). Naturally-derived biopolymers: Potential platforms for enzyme immobilization. *International Journal of Biological Macromolecules, 130*, 462–482. https://doi.org/10.1016/J.IJBIOMAC.2019.02.152

Chung, Y. C., & Chen, C. Y. (2008). Antibacterial characteristics and activity of acid-soluble chitosan. *Bioresource Technology, 99*(8), 2806–2814. https://doi.org/10.1016/J.BIORTECH.2007.06.044

Coll Cárdenas, F., Andrés, S., Giannuzzi, L., & Zaritzky, N. (2011). Antimicrobial action and effects on beef quality attributes of a gaseous ozone treatment at refrigeration temperatures. *Food Control, 22*(8), 1442–1447. https://doi.org/10.1016/J.FOODCONT.2011.03.006

Costa, E. M., Silva, S., Pina, C., Tavaria, F. K., & Pintado, M. M. (2012). Evaluation and insights into chitosan antimicrobial activity against anaerobic oral pathogens. *Anaerobe, 18*(3), 305–309. https://doi.org/10.1016/J.ANAEROBE.2012.04.009

Elsamadony, M., Elreedy, A., Mostafa, A., Fujii, M., Gescher, J., Shakeri Yekta, S., … Pant, D. (2021). Perspectives on potential applications of nanometal derivatives in gaseous bioenergy pathways: Mechanisms, life cycle, and toxicity. *ACS Sustainable Chemistry & Engineering, 9*(29), 9563–9589. https://doi.org/10.1021/ACSSUSCHEMENG.1C02260/ASSET/IMAGES/MEDIUM/SC1C02260_0014.GIF

European Pharmacopoeia. (2019). (Ph. Eur.) 10th edition | EDQM - European Directorate for the quality of medicines (n.d.). Retrieved January 22, 2022, from https://www.edqm.eu/en/european-pharmacopoeia-ph-eur-10th-edition.

Gabor, D., & Tita, O. (2012). Biopolymers used in food packaging: A review. *Acta Universitatis Cibiniensis Series E: Food Technology, XVI, 2*.

Galván Márquez, I., Akuaku, J., Cruz, I., Cheetham, J., Golshani, A., & Smith, M. L. (2013). Disruption of protein synthesis as antifungal mode of action by chitosan. *International Journal of Food Microbiology, 164*(1), 108–112. https://doi.org/10.1016/J.IJFOODMICRO.2013.03.025

Ganan, M., Carrascosa, A. V., & Martínez-Rodríguez, A. J. (2009). Antimicrobial activity of chitosan against campylobacter spp. and other microorganisms and its mechanism of action. *Journal of Food Protection, 72*(8), 1735–1738. https://doi.org/10.4315/0362-028X-72.8.1735

Ganguly, P., Breen, A., & Pillai, S. C. (2018). Toxicity of nanomaterials: Exposure, pathways, assessment, and recent advances. *ACS Biomaterials Science & Engineering*. https://doi.org/10.1021/ACSBIOMATERIALS.8B00068

Garavand, F., Rouhi, M., Razavi, S. H., Cacciotti, I., & Mohammadi, R. (2017). Improving the integrity of natural biopolymer films used in food packaging by crosslinking approach: A review. *International Journal of Biological Macromolecules, 104*, 687–707. https://doi.org/10.1016/J.IJBIOMAC.2017.06.093

Giteru, S. G., Coorey, R., Bertolatti, D., Watkin, E., Johnson, S., & Fang, Z. (2015). Physicochemical and antimicrobial properties of citral and quercetin incorporated kafirin-based bioactive films. *Food Chemistry, 168*, 341–347. https://doi.org/10.1016/J.FOODCHEM.2014.07.077

Giuliani, G., Ricevuti, G., Galoforo, A., & Franzini, M. (2018). Microbiological aspects of ozone: Bactericidal activity and antibiotic/antimicrobial resistance in bacterial strains treated with ozone. *Ozone Therapy, 3*(3). https://doi.org/10.4081/ozone.2018.7971

Gómez-Estaca, J., López de Lacey, A., López-Caballero, M. E., Gómez-Guillén, M. C., & Montero, P. (2010). Biodegradable gelatin-chitosan films incorporated with essential oils as antimicrobial agents for fish preservation. *Food Microbiology, 27*(7), 889–896. https://doi.org/10.1016/J.FM.2010.05.012

Grujić, R., Vujadinović, D., Savanović, D., Grujić, R., Vujadinović, Á. D., & Savanović, D. (2017). Biopolymers as food packaging materials. *Advances in Applications of Industrial Biomaterials, 139–160*. https://doi.org/10.1007/978-3-319-62767-0_8

Habibi Najafi, M. B., & Haddad Khodaparast, M. H. (2009). Efficacy of ozone to reduce microbial populations in date fruits. *Food Control, 20*(1), 27–30. https://doi.org/10.1016/J.FOODCONT.2008.01.010

Hm, L., Mh, K., Yi, Y., & Wh, P. (2017). Fluorescent property of chitosan oligomer and its application as a metal ion sensor. *Marine Drugs, 15*(4). https://doi.org/10.3390/MD15040105

Hudson, J. B., Sharma, M., & Vimalanathan, S. (2009). Development of a practical method for using ozone gas as a virus decontaminating agent. *31*(3), 216–223. https://doi.org/10.1080/01919510902747969

Hutchings, J. B. (1999). Food colour and appearance. *Food Colour and Appearance*. https://doi.org/10.1007/978-1-4615-2373-4

Khah, M. D., Ghanbarzadeh, B., Roufegarinejad Nezhad, L., & Ostadrahimi, A. (2021). Effects of virgin olive oil and grape seed oil on physicochemical and antimicrobial properties of pectin-gelatin blend emulsified films. *International Journal of Biological Macromolecules, 171*, 262–274. https://doi.org/10.1016/J.IJBIOMAC.2021.01.020

Khanashyam, A. C., Shanker, M. A., Kothakota, A., Mahanti, N. K., & Pandiselvam, R. (2021). Ozone applications in milk and meat industry. *44*(1), 50–65. https://doi.org/10.1080/01919512.2021.1947776

Kong, M., Chen, X. G., Xing, K., & Park, H. J. (2010). Antimicrobial properties of chitosan and mode of action: A state of the art review. *International Journal of Food Microbiology, 144*(1), 51–63. https://doi.org/10.1016/J.IJFOODMICRO.2010.09.012

Krystyjan, M., Khachatryan, G., Grabacka, M., Krzan, M., Witczak, M., Grzyb, J., & Woszczak, L. (2021). Physicochemical, bacteriostatic, and biological properties of starch/chitosan polymer composites modified by graphene oxide, designed as new bionanomaterials. *Polymers, 13*(14), 2327. https://doi.org/10.3390/POLYM13142327

Kumar, S., Mukherjee, A., & Dutta, J. (2020). Chitosan based nanocomposite films and coatings: Emerging antimicrobial food packaging alternatives. *Trends in Food Science & Technology, 97*, 196–209. https://doi.org/10.1016/J.TIFS.2020.01.002

Kumirska, J., Weinhold, M. X., Thöming, J., & Stepnowski, P. (2011). Biomedical activity of chitin/chitosan based materials—Influence of physicochemical properties apart from molecular weight and degree of N-acetylation. *Polymers, 3*(4), 1875–1901. https://doi.org/10.3390/POLYM3041875

Li, B., Wang, L., Xu, F., Gang, X., Demirci, U., Wei, D., Li, Y., Feng, Y., Jia, D., & Zhou, Y. (2015). Hydrosoluble, UV-crosslinkable and injectable chitosan for patterned cell-laden microgel and rapid transdermal curing hydrogel in vivo. *Acta Biomaterialia, 22*, 59–69. https://doi.org/10.1016/J.ACTBIO.2015.04.026

Li, C. S., & Wang, Y. C. (2010). Surface germicidal effects of ozone for microorganisms. *64*(4), 533–537. https://doi.org/10.1080/15428110308984851

Li, J., & Zhuang, S. (2020). Antibacterial activity of chitosan and its derivatives and their interaction mechanism with bacteria: Current state and perspectives. *European Polymer Journal, 138*, Article 109984. https://doi.org/10.1016/J.EURPOLYMJ.2020.109984

Liu, H., Du, Y., Wang, X., & Sun, L. (2004). Chitosan kills bacteria through cell membrane damage. *International Journal of Food Microbiology, 95*(2), 147–155. https://doi.org/10.1016/J.IJFOODMICRO.2004.01.022

Liu, N., Chen, X. G., Park, H. J., Liu, C. G., Liu, C. S., Meng, X. H., & Yu, L. J. (2006). Effect of MW and concentration of chitosan on antibacterial activity of Escherichia coli. *Carbohydrate Polymers, 64*(1), 60–65. https://doi.org/10.1016/J.CARBPOL.2005.10.028

Marangoni Júnior, L., Vieira, R. P., Jamróz, E., & Anjos, C. A. R. (2021). Furcellaran: An innovative biopolymer in the production of films and coatings. *Carbohydrate Polymers, 252*, Article 117221. https://doi.org/10.1016/J.CARBPOL.2020.117221

Mathew, S., Brahmakumar, M., & Abraham, T. E. (2006). Microstructural imaging and characterization of the mechanical, chemical, thermal, and swelling properties of starch–chitosan blend films. *Biopolymers, 82*(2), 176–187. https://doi.org/10.1002/BIP.20480

Muhlisin, M., Utama, D. T., Lee, J. H., Choi, J. H., & Lee, S. K. (2016). Effects of gaseous ozone exposure on bacterial counts and oxidative properties in chicken and duck breast meat. *Korean Journal for Food Science of Animal Resources, 36*(3), 405. https://doi.org/10.5851/KOSFA.2016.36.3.405

Olaimat, A. N., Fang, Y., & Holley, R. A. (2014). Inhibition of Campylobacter jejuni on fresh chicken breasts by κ-carrageenan/chitosan-based coatings containing allyl isothiocyanate or deodorized oriental mustard extract. *International Journal of Food Microbiology, 187*, 77–82. https://doi.org/10.1016/J.IJFOODMICRO.2014.07.003

Ortiz-Duarte, G., Martínez-Hernández, G. B., Casillas-Peñuelas, R., & Pérez-Cabrera, L. E. (2021). Evaluation of biopolymer films containing silver–chitosan nanocomposites. *Food and Bioprocess Technology, 14*(3), 492–504. https://doi.org/10.1007/S11947-021-02585-3/FIGURES/7

Park, H. J., Weller, C. L., Vergano, P. J., & Testin, R. F. (1993). Permeability and mechanical properties of cellulose-based edible films. *Journal of Food Science, 58*(6), 1361–1364. https://doi.org/10.1111/J.1365-2621.1993.TB06183.X

Park, S. C., Nah, J. W., & Park, Y. (2011). pH-dependent mode of antibacterial actions of low molecular weight water-soluble chitosan (LMWSC) against various pathogens. *Macromolecular Research, 19*(8), 853–860. https://doi.org/10.1007/S13233-011-0812-1

Pastor, C., Sánchez-González, L., Chiralt, A., Cháfer, M., & González-Martínez, C. (2013). Physical and antioxidant properties of chitosan and methylcellulose based films containing resveratrol. *Food Hydrocolloids, 30*(1), 272–280. https://doi.org/10.1016/J.FOODHYD.2012.05.026

Peng, Y., & Li, Y. (2014). Combined effects of two kinds of essential oils on physical, mechanical and structural properties of chitosan films. *Food Hydrocolloids, 36*, 287–293. https://doi.org/10.1016/J.FOODHYD.2013.10.013

Piachin, T., & Trachoo, N. (2011). Effect of ozone and potassium lactate on lipid oxidation and survival of salmonella typhimurium on fresh pork. *Pakistan Journal of Biological Sciences, 14*(3), 236–240. https://doi.org/10.3923/PJBS.2011.236.240

Qin, Y., Li, P., & Guo, Z. (2020). Cationic chitosan derivatives as potential antifungals: A review of structural optimization and applications. *Carbohydrate Polymers, 236*, Article 116002. https://doi.org/10.1016/J.CARBPOL.2020.116002

Rajabi, H. R., Shamsipur, M., Khosravi, A. A., Khani, O., & Yousefi, M. H. (2013). Selective spectrofluorimetric determination of sulfide ion using manganese doped ZnS quantum dots as luminescent probe. *Spectrochimica Acta - Part A: Molecular and Biomolecular Spectroscopy, 107*, 256–262. https://doi.org/10.1016/J.SAA.2013.01.045

Rey, R. P., Núñez Sellés, A., Baluja, C., & Lorenzo Otero, M. (2008). Ozonation kinetics of glucosamine and N-acetyl glucosamine in aqueous medium. *17*(4), 463–467. https://doi.org/10.1080/01919519508547349

Rodríguez-Rojas, A., Arango Ospina, A., Rodríguez-Vélez, P., & Arana-Florez, R. (2019). What is the new about food packaging material? A bibliometric review during 1996–2016. *Trends in Food Science & Technology, 85*, 252–261. https://doi.org/10.1016/J.TIFS.2019.01.016

Rozilah, A., Aiza Jaafar, C. N., Sapuan, S. M., Zainol, I., & Ilyas, R. A. (2020). The effects of silver nanoparticles compositions on the mechanical, physiochemical, antibacterial, and morphology properties of sugar palm starch biocomposites for antibacterial coating. *Polymers, 12*(11), 2605. https://doi.org/10.3390/POLYM12112605

Rudawska, A., & Jacniacka, E. (2009). Analysis for determining surface free energy uncertainty by the Owen-Wendt method. *International Journal of Adhesion and Adhesives, 29*(4), 451–457. https://doi.org/10.1016/j.ijadhadh.2008.09.008

Sadowska, J., Johansson, B., Johannessen, E., Friman, R., Broniarz-Press, L., & Rosenholm, J. B. (2008). Characterization of ozonated vegetable oils by spectroscopic and chromatographic methods. *Chemistry and Physics of Lipids, 151*(2), 85–91. https://doi.org/10.1016/J.CHEMPHYSLIP.2007.10.004

Sánchez-González, L., Vargas, M., González-Martínez, C., Chiralt, A., & Cháfer, M. (2009). Characterization of edible films based on hydroxypropylmethylcellulose and tea tree essential oil. *Food Hydrocolloids, 23*(8), 2102–2109. https://doi.org/10.1016/J.FOODHYD.2009.05.006

Sanuja, S., Agalya, A., & Umapathy, M. J. (2015). Synthesis and characterization of zinc oxide–neem oil–chitosan bionanocomposite for food packaging application. *International Journal of Biological Macromolecules, 74*, 76–84. https://doi.org/10.1016/J.IJBIOMAC.2014.11.036

Saral Sarojini, K., Indumathi, M. P., & Rajarajeswari, G. R. (2019). Mahua oil-based polyurethane/chitosan/nano ZnO composite films for biodegradable food packaging applications. *International Journal of Biological Macromolecules, 124*, 163–174. https://doi.org/10.1016/J.IJBIOMAC.2018.11.195

Sarkar, B., Mahanty, A., Gupta, S. K., Choudhury, A. R., Daware, A., & Bhattacharjee, S. (2022). Nanotechnology: A next-generation tool for sustainable aquaculture. *Aquaculture, 546*, Article 737330. https://doi.org/10.1016/J.AQUACULTURE.2021.737330

Sechi, L. A., Lezcano, I., Nunez, N., Espim, M., Duprè, I., Pinna, A., … Zanetti, S. (2001). Antibacterial activity of ozonized sunflower oil (Oleozon). *Journal of Applied Microbiology, 90*(2), 279–284. https://doi.org/10.1046/J.1365-2672.2001.01235.X

Serio, F., Pizzolante, G., Cozzolino, G., D'Alba, M., Bagordo, F., De Giorgi, M., … De Donno, A. (2017). A new formulation based on ozonated sunflower seed oil: In vitro antibacterial and safety evaluation. *39*(3), 139–147. https://doi.org/10.1080/01919512.2016.1272405

Siripatrawan, U. (2016). Active food packaging from chitosan incorporated with plant polyphenols. *Novel Approaches of Nanotechnology in Food, 465–507*. https://doi.org/10.1016/B978-0-12-804308-0.00014-5

Southgate, D.A.T. AFRC Institute of Food Research, Norwich Laboratory, N. United K. (1991). *Determination of food carbohydrates. ed. 2*.

Stivarius, M. R., Pohlman, F. W., McElyea, K. S., & Apple, J. K. (2002). Microbial, instrumental color and sensory color and odor characteristics of ground beef produced from beef trimmings treated with ozone or chlorine dioxide. *Meat Science, 60*(3), 299–305. https://doi.org/10.1016/S0309-1740(01)00139-5

Tseng, C. C., & Li, C. S. (2006). Ozone for inactivation of aerosolized bacteriophages. *40*(9), 683–689. https://doi.org/10.1080/02786820600796590

Udayakumar, G. P., Muthusamy, S., Selvaganesh, B., Sivarajasekar, N., Rambabu, K., Banat, F., … Show, P. L. (2021). Biopolymers and composites: Properties, characterization and their applications in food, medical and pharmaceutical industries. *Journal of Environmental Chemical Engineering, 9*(4), Article 105322. https://doi.org/10.1016/J.JECE.2021.105322

Ugazio, E., Tullio, V., Binello, A., Tagliapietra, S., & Dosio, F. (2020). Ozonated oils as antimicrobial systems in topical applications. Their characterization, current applications, and advances in improved delivery techniques. *Molecules, 25*(2), 334. https://doi.org/10.3390/MOLECULES25020334

Valizadeh, S., Naseri, M., Babaei, S., Hosseini, S. M. H., & Imani, A. (2019). Development of bioactive composite films from chitosan and carboxymethyl cellulose using glutaraldehyde, cinnamon essential oil and oleic acid. *International Journal of Biological Macromolecules, 134*, 604–612. https://doi.org/10.1016/J.IJBIOMAC.2019.05.071

Varghese, S. A., Siengchin, S., & Parameswaranpillai, J. (2020). Essential oils as antimicrobial agents in biopolymer-based food packaging - a comprehensive review. *Food Bioscience, 38*, Article 100785. https://doi.org/10.1016/J.FBIO.2020.100785

Wang, L., Li, B., Xu, F., Li, Y., Xu, Z., Wei, D., Feng, Y., Wang, Y., Jia, D., & Zhou, Y. (2017). Visual in vivo degradation of injectable hydrogel by real-time and non-invasive tracking using carbon nanodots as fluorescent indicator. *Biomaterials, 145*, 192–206. https://doi.org/10.1016/J.BIOMATERIALS.2017.08.039

Wu, M., Long, Z., Xiao, H., & Dong, C. (2016). Recent research progress on preparation and application of N, N, N-trimethyl chitosan. *Carbohydrate Research, 434*, 27–32. https://doi.org/10.1016/J.CARRES.2016.08.002

Xu, T., Gao, C. C., Feng, X., Yang, Y., Shen, X., & Tang, X. (2019). Structure, physical and antioxidant properties of chitosan-gum arabic edible films incorporated with cinnamon essential oil. *International Journal of Biological Macromolecules, 134*, 230–236. https://doi.org/10.1016/J.IJBIOMAC.2019.04.189

Yahya, E. B., Jummaat, F., Amirul, A. A., Adnan, A. S., Olaiya, N. G., Abdullah, C. K., … Abdul Khalil, H. P. S. (2020). A review on revolutionary natural biopolymer-based aerogels for antibacterial delivery. *Antibiotics, 9*(10), 648. https://doi.org/10.3390/ANTIBIOTICS9100648

Yong, H., & Liu, J. (2021). Active packaging films and edible coatings based on polyphenol-rich propolis extract: A review. *Comprehensive Reviews in Food Science and Food Safety, 20*(2), 2106–2145. https://doi.org/10.1111/1541-4337.12697

Yu, Z., Li, B., Chu, J., & Zhang, P. (2018). Silica in situ enhanced PVA/chitosan biodegradable films for food packages. *Carbohydrate Polymers, 184*, 214–220. https://doi.org/10.1016/J.CARBPOL.2017.12.043

Zhu, Y., Liu, X., Hu, Y., Wang, R., Chen, M., Wu, J., Wang, Y., Kang, S., Sun, Y., & Zhu, M. (2019). Behavior, remediation effect and toxicity of nanomaterials in water environments. *Environmental Research, 174*, 54–60. https://doi.org/10.1016/J.ENVRES.2019.04.014